CHAOS
Theory and Applications
in Applied Sciences and Engineering

e-ISSN: 2687-4539
RESEARCH ARTICLE
Vol.5 / No.1 / 2023 / pp.11-19
https://doi.org/10.51537/chaos.1204481

Chaos in a Pendulum Adaptive Frequency Oscillator Circuit Experiment

XiaoFu Li[⋆,1], **Aubrey N. Beal**[β,2], **Robert N. Dean**[α,3] **and Edmon Perkins**[⋆,4]

[⋆]LAB2701, Atwood, OK 74827, USA, [β]Dept. of Electrical & Computer Engineering, University of Alabama in Huntsville, Huntsville, AL 35899, USA, [α]Dept. of Electrical & Computer Engineering, Auburn University, Auburn, AL 36849, USA.

ABSTRACT Adaptive oscillators can learn and encode information in dynamic, plastic states. The pendulum has recently been proposed as the base oscillator of an adaptive system. In a mechanical setup, the horizontally forced pendulum adaptive frequency oscillator seeks a resonance condition by modifying the length of the pendulum's rod. This system stores the external forcing frequency when the external amplitude is small, while it can store the resonance frequency, which is affected by the nonlinearity of the pendulum, when the external amplitude is large. Furthermore, for some frequency ranges, the pendulum adaptive frequency oscillator can exhibit chaotic motion when the amplitudes are large. This adaptive oscillator could be used as a smart vibratory energy harvester device, but this chaotic region could degrade its performance by using supplementary energy to modify the rod length. The pendulum adaptive frequency oscillator's equations of motions are discussed, and a field-programmable analog array is used as an experimental realization of this system as an electronic circuit. Bifurcation diagrams are shown for both the numerical simulations and experiments, while period-3 motion is shown for the numerical simulations. As little work has been done on the stability of adaptive oscillators, the authors believe that this work is the first demonstration of chaos in an adaptive oscillator.

KEYWORDS
Adaptive oscillator
Nonlinear dynamics
Bifurcation diagrams
Field-programmable analog array
Chaotic circuits

INTRODUCTION

Adaptive oscillators were inspired by the synchronization of networks of neurons (Kempter *et al.* 1999). Dynamic Hebbian learning has been employed to encode the frequency in a plastic state of adaptive oscillators (Righetti *et al.* 2006). These plastic states are dynamic states, and the DC offset values of these plastic states correspond to information learned from an external signal. For instance, an adaptive frequency oscillator is composed of a base oscillator and a plastic frequency state, which can learn and store an external forcing frequency. Adaptive oscillators have been proposed as analog frequency analyzers (Buchli *et al.* 2008; Corron 2022) and controllers for robotic gait (Righetti *et al.* 2009). There are relatively few experimental results for adaptive oscillators, but a 4-state adaptive Hopf oscillator was implemented as an analog circuit (Li *et al.* 2021a) and a 3-state adaptive oscillator was implemented as a digital circuit (Maleki *et al.* 2015). The effects of noise on adaptive oscillators was studied with the full Fokker-Planck equation with comparisons to a physical experiment (Li *et al.* 2021b) and with a simplified Fokker-Planck equation (Buchli *et al.* 2008).

The learning tasks for adaptive oscillators are embedded in the plastic dynamic states of the system. However, oscillators are capable of other types of computation as well, even without adaptive states. For instance, the classical, non-adaptive Hopf oscillator can be realized as a powerful, reconfigurable reservoir computer (Shougat *et al.* 2021b, 2022). In this reservoir computing architecture, the physics of the oscillator are utilized as a computational resource through machine learning. Interestingly, reservoir computers can exhibit chaotic behavior as well, such as topological mixing that was observed in the Duffing array reservoir computer (Shougat *et al.* 2021a).

Manuscript received: 23 November 2022,
Revised: 16 January 2023,
Accepted: 25 January 2023.

[1] xfxyyh0812@gmail.com
[2] aubrey.beal@uah.edu
[3] deanron@auburn.edu
[4] edmon@lab2701.com (**Corresponding Author**)

Adaptive frequency oscillators are similar to Kuramoto phase oscillators (Acebrón *et al.* 2005; Xu and Jin 2012; Makarov *et al.* 2016; Dénes *et al.* 2021, 2019) and phase-locked loops (PLLs) (Métivier *et al.* 2020; Dürig *et al.* 1997; Kuznetsov *et al.* 2017) since they are capable of learning an external forcing frequency. However, in the literature, adaptive oscillators are usually constructed from a nonlinear oscillator by including the addition of dynamic, plastic states. Although chaos has been exhibited by Kuramoto arrays (Bick *et al.* 2018) and PLLs (Olson *et al.* 2011; Banerjee *et al.* 2014; Paul and Banerjee 2019; Chakraborty *et al.* 2016; Zhao *et al.* 2009; Harb and Harb 2004; Piqueira 2017) chaos has not been explored in adaptive oscillators to the authors' knowledge.

The forced single pendulum (d'Humieres *et al.* 1982; Xu *et al.* 2005; Bishop *et al.* 2005) and the unforced double pendulum were two of the prototypical systems that can exhibit chaos (Shinbrot *et al.* 1992; Levien and Tan 1993; Stachowiak and Okada 2006). Chaos synchronization between a controlled pendulum and Duffing oscillator was studied analytically (Luo and Min 2011). The energy localization phenomenon and stability for an array of coupled pendulums was investigated under different forcing conditions (Jallouli *et al.* 2017). Similar to the present work, the complete bifurcation characteristics of a rotating pendulum under nonlinear perturbation was found (Han and Cao 2016). A numerical investigation of an inverted pendulum on varying the base forcing amplitude displays the transition to chaos via an infinite sequence of period-doubling bifurcations (Kim and Hu 1998).

The extensible pendulum, where the pendulum's rod is modeled as an extensible spring, can also exhibit chaos (Nunez-Yepez *et al.* 1990). The bifurcation diagram was found for a mechanical, forced pendulum experiment (de Paula *et al.* 2006) and a forced torsional pendulum (Miao *et al.* 2014). An array of coupled nonlinear pendulum oscillators was studied to determine the effect of damping, the size of the ensemble, and the local coupling strength on its chaotic response (Munyaev *et al.* 2021). Since the pendulum is a relatively simple system that exhibits chaos, it has been used to test chaotic controllers (Pereira-Pinto *et al.* 2004; Wang and Jing 2004).

Of relevance to the current paper, the authors proposed a mechanical pendulum adaptive frequency oscillator, whose rod length is a dynamic state (Li *et al.* 2022). Instead of the adaptive frequency state learning the external forcing frequency, it was found that this type of adaptive oscillator instead learns a *resonance condition*, which maximizes the displacement of the amplitude of the pendulum. This resonance-tracking quality could make it an excellent candidate as a vibratory energy harvester. Importantly, it was observed that the pendulum adaptive frequency oscillator can exhibit chaotic motion, but the mechanical system could not explore the range of values causing this behavior. In this current paper, the pendulum adaptive frequency oscillator was implemented on a field-programmable analog array circuit, which is capable of operating at a range of parameters that exhibit chaos.

Circuit implementations of chaotic systems are widely used, such as realizations of a three-state chaotic flow (Pham *et al.* 2019), a jerk oscillator (Harrison *et al.* 2022; Rhea *et al.* 2020; Nana *et al.* 2009), a nonlinear feedback control input-introduced memristor chaotic oscillator (Lai *et al.* 2020), a novel autonomous four-dimensional hyperjerk system with hyperbolic sine nonlinearity (Leutcho *et al.* 2018), a fractional-order-based chaos system (Ouannas *et al.* 2017), a three-state chaotic system with applications to robotic navigation (Nwachioma and Pérez-Cruz 2021), and a snap system with adjustable symmetry and nonlinearity (Leutcho and Kengne 2018).

Although most papers report either simulated or experimental bifurcation diagrams, some work has compared simulated bifurcation diagrams with experimental bifurcation diagrams directly, such as a circuit implementation of the Rössler system (Ricco *et al.* 2016), an analog system realization of a time-delay chaotic oscillator (Biswas and Banerjee 2016), a Chua's circuit (Viana Jr *et al.* 2010), and a physical circuit realization of a four-dimensional chaotic system (Jahanshahi *et al.* 2021). In the current paper, both the bifurcation diagrams from numerical simulations and from the experiments are compared. For the experimental work, the pendulum adaptive frequency oscillator equations are implemented as an electronic circuit by utilizing a field-programmable analog array. The authors believe that this is the first time that chaos has been demonstrated in an adaptive oscillator and that this is the first circuit implementation of this pendulum adaptive frequency oscillator.

EQUATION OF MOTION OF HORIZONTALLY FORCED PENDULUM ADAPTIVE FREQUENCY OSCILLATOR

Table 1 List of parameters and states.

Symbol	Description
a	Forcing amplitude
k_ω	Coupling in ω state
c	Damping
l	Pendulum length
m	Mass
g	Acceleration due to gravity
Ω	External sinusoidal forcing frequency
θ	Angular position of pendulum
$\dot{\theta}$	Angular velocity of pendulum
$x(t)$	Angular position in state space
$y(t)$	Angular velocity in state space
$\omega(t)$	Adaptive frequency

In Fig. 1, the horizontally forced pendulum is depicted. In this pendulum, it is assumed that the rod is inelastic, and the horizontal forcing kinematically moves the pivot point. For reference, the constants and states are listed in Table 1. By using Lagrange's equations and assuming a Rayleigh dissipation of the form $\frac{1}{2}cml^2\dot{\theta}^2$, the governing equation can be written as follows:

$$ml^2\ddot{\theta} + cml^2\dot{\theta} + mgl\sin(\theta) = l\cos(\theta)f(t) \tag{1}$$

After dividing both sides of the equation by ml^2, eq. (1) becomes:

$$\ddot{\theta} + c\dot{\theta} + \omega_n^2\sin(\theta) = \frac{1}{ml}\cos(\theta)f(t) \tag{2}$$

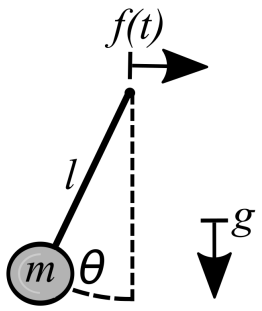

Figure 1 Pendulum with horizontal forcing, which kinematically moves the pivot point.

Converting eq. (2) into state space with $x = \theta$ and $y = \dot{\theta}$, the following set of ordinary differential equations may be written:

$$\begin{aligned} \dot{x}(t) &= y(t) \\ \dot{y}(t) &= -cy(t) - \omega_n^2 \sin\left(x(t)\right) + \frac{1}{ml}\cos\left(x(t)\right) f(t) \end{aligned} \tag{3}$$

Setting $f(t) = \hat{a}\sin\left(\Omega t\right)$ with $\hat{a} = aml$, eq. (3) can be written as:

$$\begin{aligned} \dot{x}(t) &= y(t) \\ \dot{y}(t) &= -cy(t) - \omega_n^2 \sin\left(x(t)\right) + a\cos\left(x(t)\right)\sin\left(\Omega t\right) \end{aligned} \tag{4}$$

Here, a is the amplitude of the sinusoidal forcing. Using these pendulum equations as a base oscillator, a pendulum adaptive frequency oscillator can be constructed by adding a plastic, dynamic state that can learn the external forcing frequency:

$$\begin{aligned} \dot{x}(t) &= y(t) \\ \dot{y}(t) &= -cy(t) - \omega^2(t)\sin\left(x(t)\right) + a\cos\left(x(t)\right)\sin\left(\Omega t\right) \\ \dot{\omega}(t) &= \frac{-k_\omega x(t) a \sin\left(\Omega t\right)}{\sqrt{x^2(t)+y^2(t)}} \end{aligned} \tag{5}$$

The $\dot{\omega}$ equation is responsible for learning and storing the external frequency in the ω state. The right-hand side of this equation is a mixture of two time-varying signals, $x(t)$ and $a\sin\left(\Omega t\right)$. When the system is not undergoing chaotic motion, $x(t)$ becomes entrained to the external sinusoid, which causes the ω state to converge to Ω. The right-hand side of this equation is also normalized by the amplitude of the cyclic motion of the pendulum, $\sqrt{x^2(t)+y^2(t)}$. k_ω is the coupling strength in this third state.

It should also be noted that the damped pendulum (eq. (4)) does not have an analytical solution (Gitterman 2010). By extension, it is very unlikely that the damped adaptive pendulum (eq. (5)) would have an analytical solution either. For this reason, numerical simulations and experiments are used to exhibit chaos in this adaptive oscillator.

When eq. (5) is in a regime in which it correctly learns the external forcing frequency, a local stability analysis can be constructed. For this analysis, the external sinusoid can be replaced with an additional oscillator to convert eq. (5) into an autonomous system (Perkins 2019). When this additional oscillator undergoes a supercritical Andronov-Hopf bifurcation, it resonates with a frequency of Ω Perkins and Fitzgerald (2018). The set of autonomous equations can be written as:

$$\begin{aligned} \dot{x}(t) &= y(t) \\ \dot{y}(t) &= -cy(t) - \omega^2(t)\sin\left(x(t)\right) + a\cos\left(x(t)\right)u \\ \dot{\omega}(t) &= \frac{-k_\omega x(t) a u}{\sqrt{x^2(t)+y^2(t)}} \\ \dot{u} &= u + \Omega v - u(u^2+v^2) \\ \dot{v} &= v - \Omega u - v(u^2+v^2) \end{aligned} \tag{6}$$

Here, the last two equations represent the additional oscillator. The Jacobian, J, for eq. (6) may be written as:

$$J = \begin{bmatrix} 0 & j_1 & 0 & 0 & 0 \\ j_2 & j_3 & j_4 & j_5 & 0 \\ j_6 & j_7 & 0 & j_8 & 0 \\ 0 & 0 & 0 & j_9 & j_{10} \\ 0 & 0 & 0 & j_{11} & j_{12} \end{bmatrix} \tag{7}$$

The elements for this Jacobian are: $j_1 = 1$, $j_2 = -\omega^2\cos\left(x\right) - au\sin\left(x\right)$, $j_3 = -c$, $j_4 = -2\omega\sin\left(x\right)$, $j_5 = a\cos\left(x\right)$, $j_6 = \frac{ak_\omega u x^2}{(x^2+y^2)^{\frac{3}{2}}} - \frac{ak_\omega u}{(x^2+y^2)^{\frac{1}{2}}}$, $j_7 = \frac{ak_\omega u x y}{(x^2+y^2)^{\frac{3}{2}}}$, $j_8 = \frac{-ak_\omega x}{(x^2+y^2)^{\frac{3}{2}}}$, $j_9 = 1 - 3u^2 - v^2$, $j_{10} = -2uv + \Omega$, $j_{11} = -2uv - \Omega$, and $j_{12} = 1 - u^2 - 3v^2$. For the fixed point $(x, y, u, v) = (2\pi, 0, 0, 0)$, the eigenvalues for the Jacobian are $1 \pm i\Omega$, $\frac{-c\pm\sqrt{c^2-4\omega^2}}{2}$, and 0. The first conjugate pair, $1 \pm i\Omega$, corresponds to the additional oscillator, which oscillates at a frequency of Ω.

The second conjugate pair is $\frac{-c\pm\sqrt{c^2-4\omega^2}}{2}$. Noting that eq. (4) is a pendulum with an effective mass equal to 1, we may rewrite this conjugate pair of eigenvalues as $-\zeta\omega_n \pm i\omega_n\sqrt{1-\zeta^2}$. Here, ζ is the damping factor and ω_n is the linear natural frequency of the pendulum. Thus, the second conjugate pair of eigenvalues corresponds to the damped pendulum, which oscillates at the damped natural frequency, $\omega_d = \omega_n\sqrt{1-\zeta^2}$. The last eigenvalue, 0, corresponds to the ω state. This state is neither stable nor unstable, which allows it to deform to the external forcing frequency.

SIMULATION RESULTS

For most values of the forcing frequency, Ω, the pendulum adaptive frequency oscillator behaves as expected: the frequency state converges to the forcing frequency. This behavior is depicted in Fig. 2. For this figure and for the subsequent bifurcation diagrams, a quasi-static frequency sweep was performed, for both the numerical simulations and the experiments. In Figs. 2 and 3, *ode45* in MATLAB was used to simulate eq. (5) for 400 periods of the forcing function, $\sin\left(\Omega t\right)$. Only the last 100 cycles were used to create Figs. 2 and 3, to avoid any transient behavior. Poincaré sections were taken of the pendulum's dynamics, using the external sinusoid as the clock with frequency Ω.

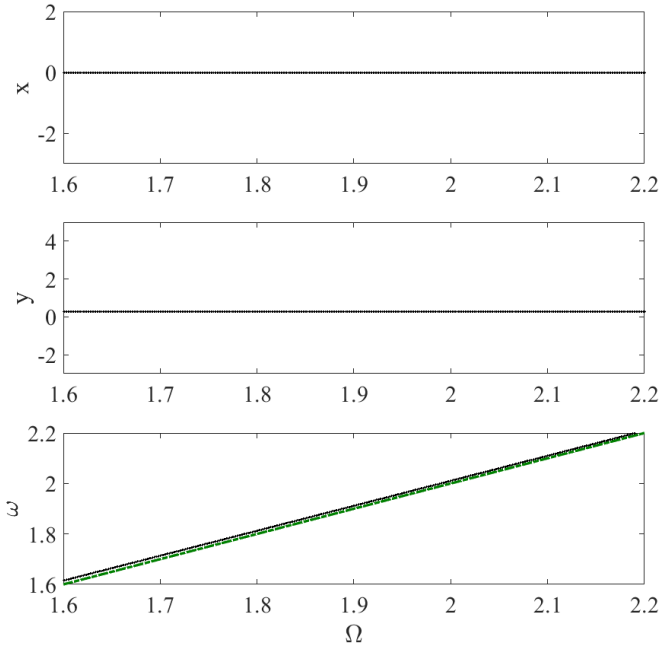

Figure 2 Poincaré sections of the states of the horizontally forced pendulum adaptive frequency oscillator for Ω ranging from 1.6 rad/s to 2.2 rad/s. Here, $a = 0.1$, $c = 0.35$, and $k_\omega = 0.707$. The green dashed line represents the line $\omega = \Omega$. For this combination of parameters, the pendulum adaptive frequency oscillator correctly learns the external forcing frequency. This figure can be compared with the chaotic bifurcation diagram that is shown in Fig. 3.

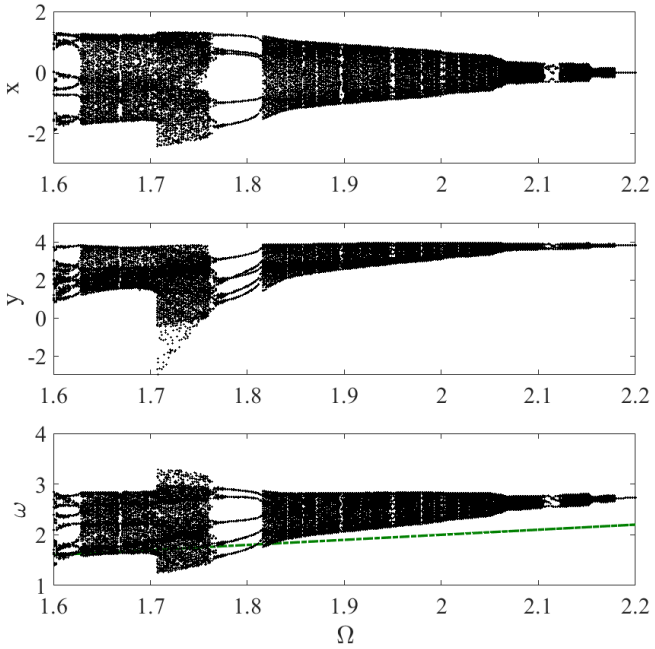

Figure 3 Bifurcation diagram using the Poincaré sections of the states of the horizontally forced pendulum adaptive frequency oscillator for Ω ranging from 1.6 rad/s to 2.2 rad/s. Here, $a = 1.8$, $c = 0.35$, and $k_\omega = 0.707$. The green dashed line represents the line $\omega = \Omega$. Instead of learning the external forcing frequency, the bifurcation diagram exhibits chaotic behavior. This figure can be compared with the non-chaotic bifurcation diagram that is shown in Fig. 2.

In Fig. 2, the pendulum adaptive frequency oscillator's Poincaré sections show that the ω state has properly learned the external forcing frequency, Ω. Since the x and y states are periodic with the same frequency as the external sinusoid, their Poincaré sections appear stationary with respect to this clock.

Repeating this same procedure that was used for Fig. 2, the bifurcation diagram is constructed, which is depicted in Fig. 3. For this set of parameters, the pendulum adaptive frequency oscillator does not properly learn the external forcing frequency. Instead, the system has a chaotic response.

Other combinations of parameters can also result in a chaotic response. Two other bifurcation diagrams are shown in Figs. 4 and 5. In these bifurcation diagrams, the k_ω (Fig. 4) and c (Fig. 5) parameters were varied to highlight that the pendulum adaptive frequency oscillator may also experience chaotic motion.

In general, these bifurcation diagrams provide some insights into a working range for the parameters of the pendulum adaptive frequency oscillator. The forcing amplitude, a, and the coupling term, k_ω, should be relatively small. A higher value of the damping, c, hinders the chaotic motion for the parameters considered here. Further, this adaptive oscillator works better when the forcing frequency, Ω, is relatively large. When the pendulum adaptive frequency oscillator is tasked with learning a low frequency response with a large amplitude, it can result in a chaotic response.

For some parameter combinations, period-3 motion may be observed, which shows that this system is indeed chaotic (Li and Yorke 2004). In Fig. 6, period-3 motion may be seen in the time history. The three dimensional trajectory of the system is shown for comparison.

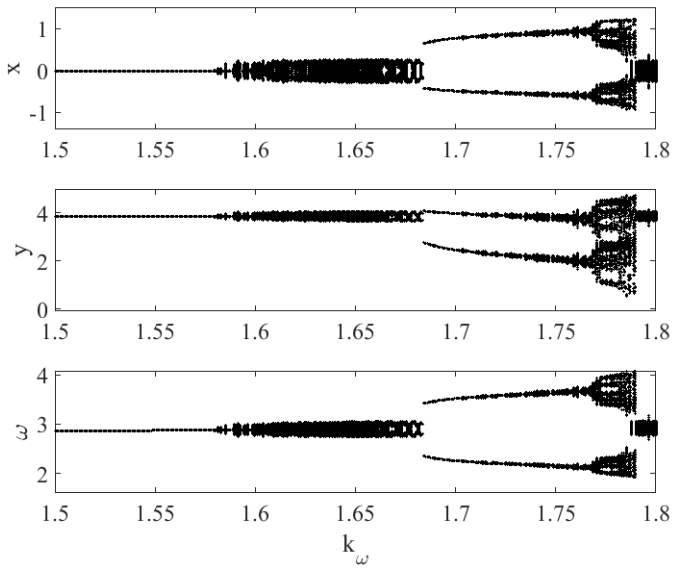

Figure 4 Bifurcation diagram using the Poincaré sections of the states of the horizontally forced pendulum adaptive frequency oscillator for k_ω ranging from 1.5 to 1.8. Here, $a = 1.8$, $c = 0.35$, and $\Omega = 2.2$ rad/s. Some of these values of k_ω can result in chaotic motion.

For other parameters, strange attractors may be observed. One of these strange attractors is depicted in Fig. 7.

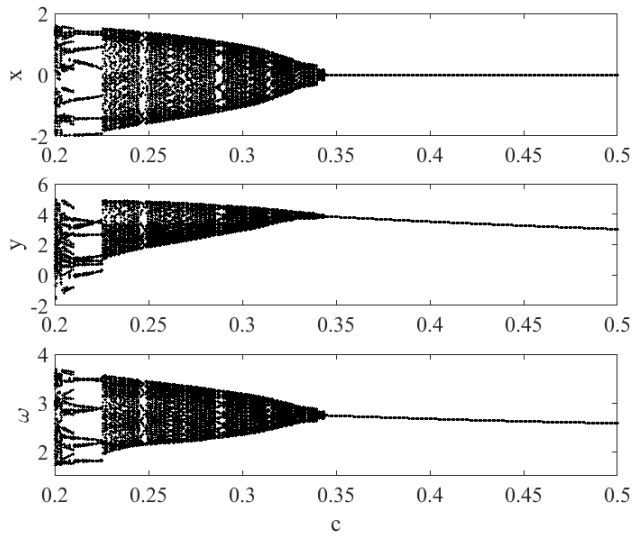

Figure 5 Bifurcation diagram using the Poincaré sections of the states of the horizontally forced pendulum adaptive frequency oscillator for c ranging from 0.2 to 0.5. Here, $a = 1.8$, $k_\omega = 0.707$, and $\Omega = 2.2$ rad/s. Some of these values of c can result in chaotic motion.

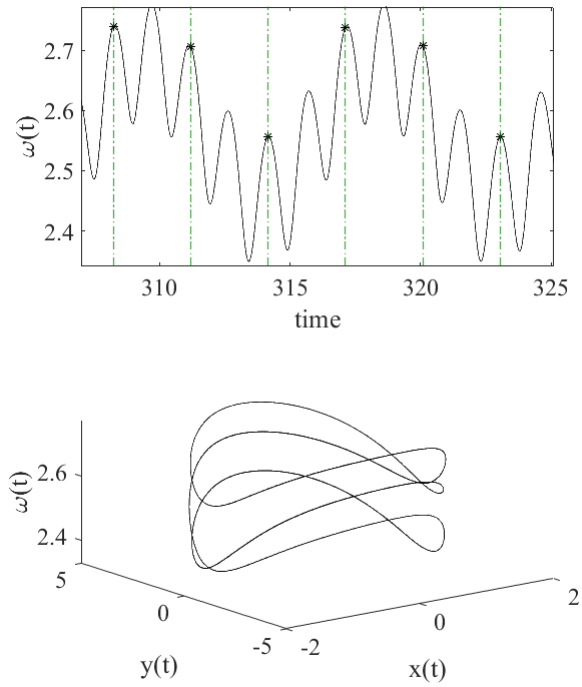

Figure 6 For $\Omega = 2.12$ rad/s, the response of the ω state has period-3 motion. Here, $a = 1.8$, $c = 0.35$, and $k_\omega = 0.707$. In the top plot, the Poincaré sections are shown for a portion of the time history. The vertical green dashed lines depict the clock's sampling rate for the stroboscope, and the * is the value of the ω state at these times. In the bottom plot, the three dimensional trajectory of the system is shown.

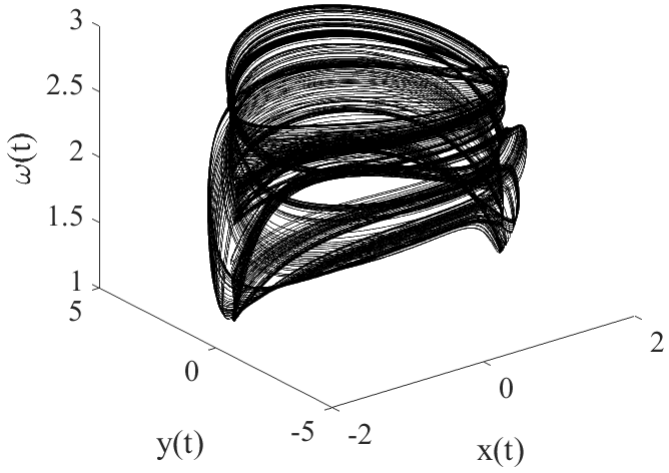

Figure 7 For $\Omega = 1.67$, a strange attractor is shown. For this simulation, $a = 1.8$, $c = 0.35$, and $k_\omega = 0.707$.

FIELD-PROGRAMMABLE ANALOG ARRAY CIRCUIT

The pendulum adaptive frequency oscillator was implemented as a field-programmable analog array circuit. Field-programmable analog arrays (FPAAs) are dynamically programmable analog signal processing devices that use switched-capacitor technology (Kutuk and Kang 1996). FPAAs contains configurable analog blocks (CABs), which create analog operations. Each math operation is further achieved by configurable analog modules (CAMs). By using FPAAs, the design of nonlinear systems are significantly reduced, as the technology is highly reconfigurable (Kilic and Dalkiran 2009).

Several FPAA implementations of nonlinear dynamical system have been widely studied, which include the implementation of the Lorenz system (Tlelo-Cuautle *et al.* 2020), a cellular network-based Lorenz-like system (Günay and Altun 2018), the Sprott N chaotic oscillator (Li *et al.* 2018; Çiçek 2019), the Nahrain chaotic map (Abdullah and Abdullah 2019), a fractional-order chaotic system (Silva-Juárez *et al.* 2020), a chaotic oscillator (Dalkiran and Sprott 2016), and the Hindmarsh–Rose Neuron model (Dahasert *et al.* 2012). As compared with printed circuit boards, FPAAs can accomplish faster prototyping, without using large amounts of operational amplifiers and analog multipliers. The nonlinear functions, such as the sinusoids and square root operation in eq. (5), can be approximated as a user-defined voltage transfer function with CAMs. Utilizing the modular design of FPAAs, this pendulum frequency adaptive oscillator is implemented as a physical experiment.

However, the FPAA's input and output must be in a range between ± 3 volts. This necessitates that the response amplitude must be rescaled. Based on the numerical time response results shown in Fig. 3, only the y state significantly exceeds the maximum voltage range of the FPAA. It should also be noted that the FPAA experiment runs at 1000 times faster than the numerical simulations, due to the RC time constant of the FPAA. Thus, new states are introduced such that $x = X$, $y = 2Y$, and $\omega = 1000W$. Using these relationships, eq. (5) is modified for use on the FPAA as follows:

$$
\begin{aligned}
\dot{X}(t) &= 2Y(t) \\
\dot{Y}(t) &= -cY(t) - \tfrac{1}{2}\left(W^2(t)\sin X(t) - a\cos\left(X(t)\right)\sin\left(\Omega t\right)\right) \\
\dot{W}(t) &= \frac{-k_\omega X(t) a \sin\left(\Omega t\right)}{1000\sqrt{X^2(t)+4Y^2(t)}}
\end{aligned}
\tag{8}
$$

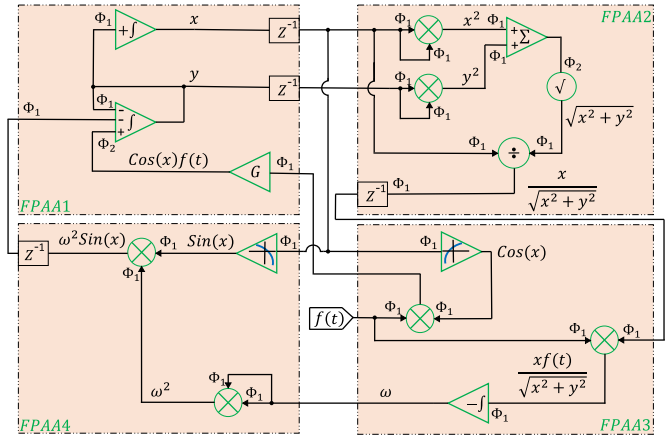

Figure 8 FPAA circuit schematic of pendulum adaptive frequency oscillator. An external forcing signal was sent to the FPAA via differential input IO3 of FPAA3.

An Anadigm Quad Apex v2.0 FPAA development board with 4 AN231E04 chips was used. The *AnadigmDesigner*2 simulator developed by Anadigm was used for FPAA hardware routing and design. All the external stimuli for the experimental results were generated in MATLAB, and they were then input to the FPAA through the differential IO cell using a National Instruments (NI) cDAQ-9174. Similarly, all the outputs of the FPAA are collected by the NI unit.

EXPERIMENTAL RESULTS

In this section, results from the FPAA pendulum adaptive frequency oscillator prototype are shown. For Figs. 9 and 10, the same procedure was used that was described for Figs. 2 and 3. A frequency sweep was performed on the FPAA analog circuit, and only the last 100 cycles were used for the Poincaré section plots in Figs. 9 and 10 to avoid any transient behavior.

In Fig. 9, the FPAA's Poincaré sections show that the ω state (where $1000 \times W = \omega$) closely learned the external forcing frequency, Ω. However, nonlinear features of the FPAA cause some errors that were not seen in the numerical simulations. Since the x and y states are periodic with the same frequency as the external sinusoid, their Poincaré sections appear stationary with respect to this clock.

Repeating this same procedure that was used for Fig. 9, the bifurcation diagram is also constructed for the FPAA, which is depicted in Fig. 10. For this set of parameters, the FPAA has a chaotic response.

In the experimental FPAA prototype, strange attractors are also present. One of these strange attractors is depicted in Fig. 11.

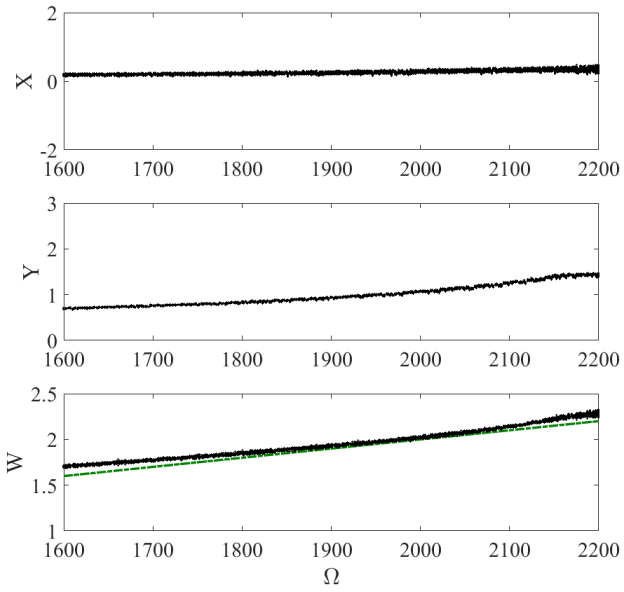

Figure 9 Poincaré sections of the states of the FPAA circuit for Ω ranging from 1600 rad/s to 2200 rad/s. Note that the FPAA runs at 1000 times faster than the simulations due to the RC time constant, so the W state should be multiplied by 1000 to calculate the learned frequency. Here, $a = 0.1$, $c = 0.35$, and $k_\omega = 0.707$. The green dashed line represents the line $\frac{\omega}{1000} = \Omega$. For this combination of parameters, the FPAA correctly learns the external forcing frequency.

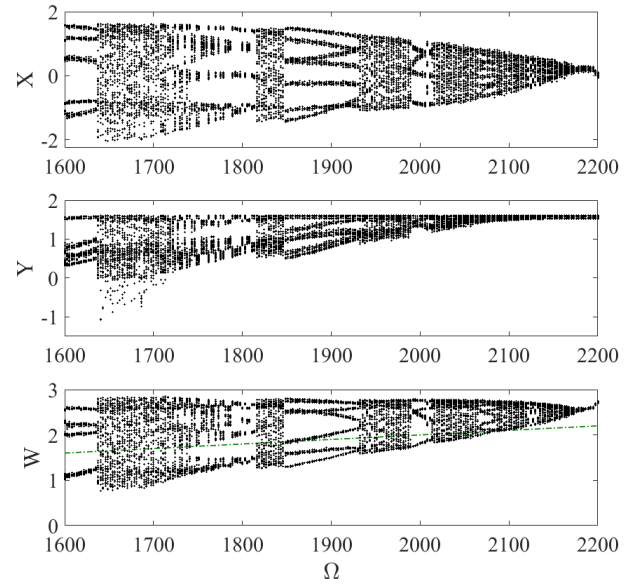

Figure 10 Bifurcation diagram using the Poincaré sections of the states of the FPAA for Ω ranging from 1600 rad/s to 2200 rad/s. Note that the FPAA runs at 1000 times faster than the simulations due to the RC time constant, so the W state should be multiplied by 1000 to calculate the learned frequency. Here, $a = 1.8$, $c = 0.35$, and $k_\omega = 0.707$. The green dashed line represents the line $\frac{\omega}{1000} = \Omega$. Instead of learning the external forcing frequency, the bifurcation diagram exhibits chaotic behavior.

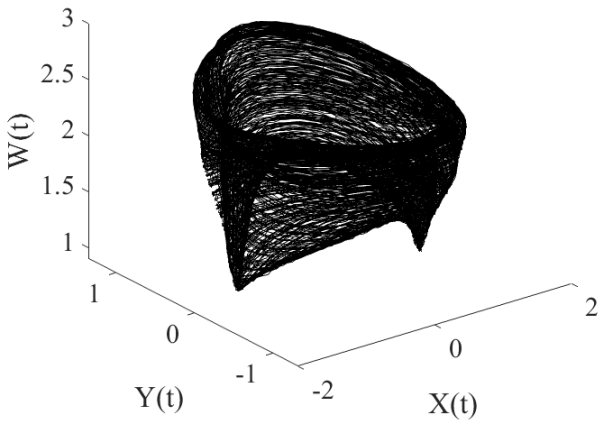

Figure 11 For $\Omega = 1640$, a strange attractor is shown. For this experiment, $a = 1.8$, $c = 0.35$, and $k_\omega = 0.707$.

Since the FPAA's frequency is scaled by 1000 from the simulations, the frequency for the strange attractor in Fig. 11 is comparable to the attractor shown in Fig. 7. Period-5 motion is depicted in Fig. 12 for the FPAA's response.

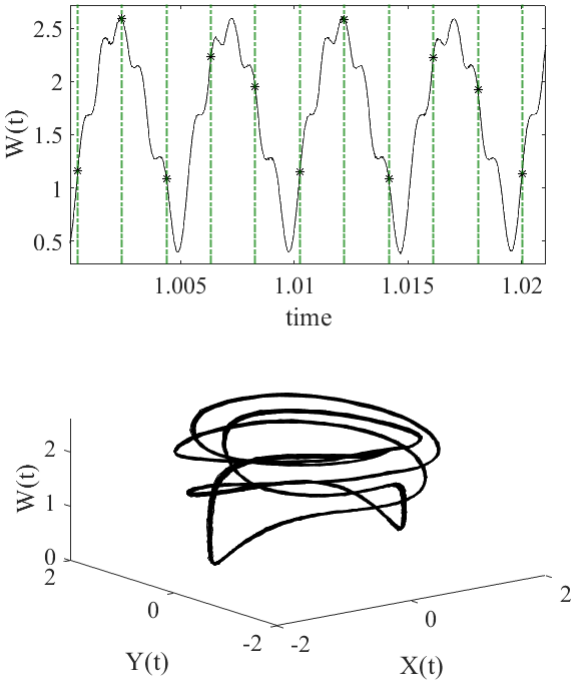

Figure 12 For $\Omega = 1880$ rad/s, the response of the W state has period-5 motion. Here, $a = 1.8$, $c = 0.35$, and $k_\omega = 0.707$. In the top plot, the Poincaré sections are shown for a portion of the time history. The vertical green dashed lines depict the clock's sampling rate for the stroboscope, and the * is the value of the W state at these times. In the bottom plot, the three dimensional trajectory of the system is shown.

CONCLUSIONS

Adaptive oscillators are a potentially useful subset of nonlinear oscillators. However, they have not been thoroughly explored. In this paper, the pendulum adaptive frequency oscillator was studied. To the authors' knowledge, this is the first circuit prototype of a pendulum adaptive frequency oscillator, and this is the first time that chaos has been observed for an adaptive oscillator. This pendulum adaptive frequency oscillator was studied through numerical simulations and a field-programmable analog array experiment. As there is interest in using a mechanical pendulum as the base oscillator (Li *et al.* 2022), this FPAA prototype provides a method of experimentally interrogating the dynamics of this system without building multiple costly mechanical prototypes.

It was found that for some parameter combinations, the pendulum adaptive frequency oscillator performed as expected in learning the external forcing frequency. At other parameter combinations, the pendulum adaptive frequency oscillator behaved chaotically. As the pendulum adaptive frequency oscillator has been proposed as a vibratory energy harvester, it is important to avoid this chaotic behavior, since the system would use energy to adapt the rod length of the pendulum.

Bifurcation diagrams were constructed for both the numerical simulations and the experiment. It should be noted that the bifurcation diagrams for the simulations and experiments were very similar, although they are not identical. Since this is a chaotic system, it is difficult to match the bifurcation diagrams of a model with an experiment, as chaotic systems have sensitive dependence on system parameters. In other words, it would be very difficult to tune the experiment's parameters to exactly match those used in the model. Strange attractors for both the simulations and experiment were also reported. Period-3 motion was found, which implies that the system is indeed chaotic.

Acknowledgments

Partial support for this project from DARPA's Young Faculty Award is greatly appreciated. Research was sponsored by the Army Research Office and was accomplished under Grant Number **W911NF-20-1-0336**. The views and conclusions contained in this document are those of the authors and should not be interpreted as representing the official policies, either expressed or implied, of the Army Research Office or the U.S. Government. The U.S. Government is authorized to reproduce and distribute reprints for Government purposes notwithstanding any copyright notation herein.

Conflicts of interest

The authors declare that there is no conflict of interest regarding the publication of this paper.

Availability of data and material

Not applicable.

LITERATURE CITED

Abdullah, H. A. and H. N. Abdullah, 2019 Design and fpaa implementation of novel chaotic system. Univ Politehnica Bucharest Scient Bull Ser C-Electrical Eng Comput Sci **81**: 153–164.

Acebrón, J. A., L. L. Bonilla, C. J. P. Vicente, F. Ritort, and R. Spigler, 2005 The kuramoto model: A simple paradigm for synchronization phenomena. Reviews of modern physics **77**: 137.

Banerjee, T., B. Paul, and B. Sarkar, 2014 Spatiotemporal dynamics of a digital phase-locked loop based coupled map lattice system.

Chaos: An Interdisciplinary Journal of Nonlinear Science **24**: 013116.

Bick, C., M. J. Panaggio, and E. A. Martens, 2018 Chaos in kuramoto oscillator networks. Chaos: An Interdisciplinary Journal of Nonlinear Science **28**: 071102.

Bishop, S., A. Sofroniou, and P. Shi, 2005 Symmetry-breaking in the response of the parametrically excited pendulum model. Chaos, Solitons & Fractals **25**: 257–264.

Biswas, D. and T. Banerjee, 2016 A simple chaotic and hyperchaotic time-delay system: design and electronic circuit implementation. Nonlinear Dynamics **83**: 2331–2347.

Buchli, J., L. Righetti, and A. J. Ijspeert, 2008 Frequency analysis with coupled nonlinear oscillators. Physica D: Nonlinear Phenomena **237**: 1705–1718.

Chakraborty, S., M. Dandapathak, and B. Sarkar, 2016 Oscillation quenching in third order phase locked loop coupled by mean field diffusive coupling. Chaos: An Interdisciplinary Journal of Nonlinear Science **26**: 113106.

Çiçek, S., 2019 Fpaa based desıgn and implementation of sprott n chaotic system. In *International Scientific and Vocational Studies Congress*, pp. 476–482, BILMES 2019 Ankara.

Corron, N. J., 2022 Complex waveform estimation using adaptive frequency oscillators. Chaos, Solitons & Fractals **158**: 111991.

Dahasert, N., İ. Öztürk, and R. Kiliç, 2012 Experimental realizations of the hr neuron model with programmable hardware and synchronization applications. Nonlinear Dynamics **70**: 2343–2358.

Dalkiran, F. Y. and J. C. Sprott, 2016 Simple chaotic hyperjerk system. International Journal of Bifurcation and Chaos **26**: 1650189.

de Paula, A. S., M. A. Savi, and F. H. I. Pereira-Pinto, 2006 Chaos and transient chaos in an experimental nonlinear pendulum. Journal of sound and vibration **294**: 585–595.

Dénes, K., B. Sándor, and Z. Néda, 2019 Pattern selection in a ring of kuramoto oscillators. Communications in Nonlinear Science and Numerical Simulation **78**: 104868.

Dénes, K., B. Sándor, and Z. Néda, 2021 Synchronization patterns in rings of time-delayed kuramoto oscillators. Communications in Nonlinear Science and Numerical Simulation **93**: 105505.

d'Humieres, D., M. Beasley, B. Huberman, and A. Libchaber, 1982 Chaotic states and routes to chaos in the forced pendulum. Physical Review A **26**: 3483.

Dürig, U., H. Steinauer, and N. Blanc, 1997 Dynamic force microscopy by means of the phase-controlled oscillator method. Journal of applied physics **82**: 3641–3651.

Gitterman, M., 2010 *The Chaotic Pendulum*. World Scientific.

Günay, E. and K. Altun, 2018 Lorenz-like system design using cellular neural networks. Turkish Journal of Electrical Engineering & Computer Sciences **26**: 1812–1819.

Han, N. and Q. Cao, 2016 Global bifurcations of a rotating pendulum with irrational nonlinearity. Communications in Nonlinear Science and Numerical Simulation **36**: 431–445.

Harb, B. A. and A. M. Harb, 2004 Chaos and bifurcation in a third-order phase locked loop. Chaos, Solitons & Fractals **19**: 667–672.

Harrison, R. C., A. OLDAG, E. PERKİNS, *et al.*, 2022 Experimental validation of a chaotic jerk circuit based true random number generator. Chaos Theory and Applications **4**: 64–70.

Jahanshahi, H., O. Orozco-López, J. M. Munoz-Pacheco, N. D. Alotaibi, C. Volos, *et al.*, 2021 Simulation and experimental validation of a non-equilibrium chaotic system. Chaos, Solitons & Fractals **143**: 110539.

Jallouli, A., N. Kacem, and N. Bouhaddi, 2017 Stabilization of solitons in coupled nonlinear pendulums with simultaneous external and parametric excitations. Communications in Nonlinear Science and Numerical Simulation **42**: 1–11.

Kempter, R., W. Gerstner, and J. L. Van Hemmen, 1999 Hebbian learning and spiking neurons. Physical Review E **59**: 4498.

Kilic, R. and F. Y. Dalkiran, 2009 Reconfigurable implementations of chua's circuit. International Journal of Bifurcation and Chaos **19**: 1339–1350.

Kim, S.-Y. and B. Hu, 1998 Bifurcations and transitions to chaos in an inverted pendulum. Physical Review E **58**: 3028.

Kutuk, H. and S.-M. Kang, 1996 A field-programmable analog array (fpaa) using switched-capacitor techniques. In *1996 IEEE International Symposium on Circuits and Systems. Circuits and Systems Connecting the World. ISCAS 96*, volume 4, pp. 41–44, IEEE.

Kuznetsov, N. V., G. A. Leonov, M. V. Yuldashev, and R. V. Yuldashev, 2017 Hidden attractors in dynamical models of phase-locked loop circuits: limitations of simulation in matlab and spice. Communications in Nonlinear Science and Numerical Simulation **51**: 39–49.

Lai, Q., Z. Wan, P. D. K. Kuate, and H. Fotsin, 2020 Coexisting attractors, circuit implementation and synchronization control of a new chaotic system evolved from the simplest memristor chaotic circuit. Communications in Nonlinear Science and Numerical Simulation **89**: 105341.

Leutcho, G., J. Kengne, and L. K. Kengne, 2018 Dynamical analysis of a novel autonomous 4-d hyperjerk circuit with hyperbolic sine nonlinearity: chaos, antimonotonicity and a plethora of coexisting attractors. Chaos, Solitons & Fractals **107**: 67–87.

Leutcho, G. D. and J. Kengne, 2018 A unique chaotic snap system with a smoothly adjustable symmetry and nonlinearity: Chaos, offset-boosting, antimonotonicity, and coexisting multiple attractors. Chaos, Solitons & Fractals **113**: 275–293.

Levien, R. and S. Tan, 1993 Double pendulum: An experiment in chaos. American Journal of Physics **61**: 1038–1044.

Li, C., W. J.-C. Thio, J. C. Sprott, H. H.-C. Iu, and Y. Xu, 2018 Constructing infinitely many attractors in a programmable chaotic circuit. IEEE Access **6**: 29003–29012.

Li, T.-Y. and J. A. Yorke, 2004 Period three implies chaos. In *The theory of chaotic attractors*, pp. 77–84, Springer.

Li, X., P. Kallepalli, T. Mollik, M. R. E. U. Shougat, S. Kennedy, *et al.*, 2022 The pendulum adaptive frequency oscillator. Mechanical Systems and Signal Processing **179**: 109361.

Li, X., M. R. E. U. Shougat, S. Kennedy, C. Fendley, R. N. Dean, *et al.*, 2021a A four-state adaptive hopf oscillator. Plos one **16**: e0249131.

Li, X., M. R. E. U. Shougat, T. Mollik, A. N. Beal, R. N. Dean, *et al.*, 2021b Stochastic effects on a hopf adaptive frequency oscillator. Journal of Applied Physics **129**: 224901.

Luo, A. C. and F. Min, 2011 The chaotic synchronization of a controlled pendulum with a periodically forced, damped duffing oscillator. Communications in Nonlinear Science and Numerical Simulation **16**: 4704–4717.

Makarov, V., A. Koronovskii, V. Maksimenko, A. Hramov, O. Moskalenko, *et al.*, 2016 Emergence of a multilayer structure in adaptive networks of phase oscillators. Chaos, Solitons & Fractals **84**: 23–30.

Maleki, M. A., A. Ahmadi, S. V. A.-D. Makki, H. Soleimani, and M. Bavandpour, 2015 Networked adaptive non-linear oscillators: a digital synthesis and application. Circuits, Systems, and Signal Processing **34**: 483–512.

Métivier, D., L. Wetzel, and S. Gupta, 2020 Onset of synchronization in networks of second-order kuramoto oscillators with delayed coupling: Exact results and application to phase-locked loops. Physical Review Research **2**: 023183.

Miao, C., W. Luo, Y. Ma, W. Liu, and J. Xiao, 2014 A simple method to improve a torsion pendulum for studying chaos. European Journal of Physics **35**: 055012.

Munyaev, V. O., D. S. Khorkin, M. I. Bolotov, L. A. Smirnov, and G. V. Osipov, 2021 Appearance of chaos and hyperchaos in evolving pendulum network. Chaos: An Interdisciplinary Journal of Nonlinear Science **31**: 063106.

Nana, B., P. Woafo, and S. Domngang, 2009 Chaotic synchronization with experimental application to secure communications. Communications in nonlinear science and Numerical Simulation **14**: 2266–2276.

Nunez-Yepez, H., A. Salas-Brito, C. Vargas, and L. Vicente, 1990 Onset of chaos in an extensible pendulum. Physics Letters A **145**: 101–105.

Nwachioma, C. and J. H. Pérez-Cruz, 2021 Analysis of a new chaotic system, electronic realization and use in navigation of differential drive mobile robot. Chaos, Solitons & Fractals **144**: 110684.

Olson, C., J. Nichols, J. Michalowicz, and F. Bucholtz, 2011 Signal design using nonlinear oscillators and evolutionary algorithms: Application to phase-locked loop disruption. Chaos: An Interdisciplinary Journal of Nonlinear Science **21**: 023136.

Ouannas, A., Z. Odibat, and T. Hayat, 2017 Fractional analysis of co-existence of some types of chaos synchronization. Chaos, Solitons & Fractals **105**: 215–223.

Paul, B. and T. Banerjee, 2019 Chimeras in digital phase-locked loops. Chaos: An Interdisciplinary Journal of Nonlinear Science **29**: 013102.

Pereira-Pinto, F. H. I., A. M. Ferreira, and M. A. Savi, 2004 Chaos control in a nonlinear pendulum using a semi-continuous method. Chaos, Solitons & Fractals **22**: 653–668.

Perkins, E., 2019 Restricted normal mode analysis and chaotic response of p-mode intrinsic localized mode. Nonlinear Dynamics **97**: 955–966.

Perkins, E. and T. Fitzgerald, 2018 Continuation method on cumulant neglect equations. Journal of Computational and Nonlinear Dynamics **13**.

Pham, V.-T., S. Jafari, C. Volos, and L. Fortuna, 2019 Simulation and experimental implementation of a line–equilibrium system without linear term. Chaos, Solitons & Fractals **120**: 213–221.

Piqueira, J. R. C., 2017 Hopf bifurcation and chaos in a third-order phase-locked loop. Communications in Nonlinear Science and Numerical Simulation **42**: 178–186.

Rhea, B. K., R. C. Harrison, F. T. Werner, E. Perkins, and R. N. Dean, 2020 Approximating an exactly solvable chaotic oscillator using a colpitts oscillator circuit. IEEE Transactions on Circuits and Systems II: Express Briefs **68**: 1028–1032.

Ricco, R. A., A. Verly, and G. F. V. Amaral, 2016 A circuit for automatic measurement of bifurcation diagram in nonlinear electronic oscillators. IEEE Latin America Transactions **14**: 3042–3047.

Righetti, L., J. Buchli, and A. J. Ijspeert, 2006 Dynamic hebbian learning in adaptive frequency oscillators. Physica D: Nonlinear Phenomena **216**: 269–281.

Righetti, L., J. Buchli, and A. J. Ijspeert, 2009 Adaptive frequency oscillators and applications. The Open Cybernetics & Systemics Journal **3**.

Shinbrot, T., C. Grebogi, J. Wisdom, and J. A. Yorke, 1992 Chaos in a double pendulum. American Journal of Physics **60**: 491–499.

Shougat, M., R. E. Ul, X. Li, T. Mollik, and E. Perkins, 2021a An information theoretic study of a duffing oscillator array reservoir computer. Journal of Computational and Nonlinear Dynamics **16**.

Shougat, M. R. E. U., X. Li, T. Mollik, and E. Perkins, 2021b A hopf physical reservoir computer. Scientific Reports **11**: 1–13.

Shougat, M. R. E. U., X. Li, and E. Perkins, 2022 Dynamic effects on reservoir computing with a hopf oscillator. Physical Review E **105**: 044212.

Silva-Juárez, A., E. Tlelo-Cuautle, L. G. de la Fraga, and R. Li, 2020 Fpaa-based implementation of fractional-order chaotic oscillators using first-order active filter blocks. Journal of advanced research .

Stachowiak, T. and T. Okada, 2006 A numerical analysis of chaos in the double pendulum. Chaos, Solitons & Fractals **29**: 417–422.

Tlelo-Cuautle, E., A. D. Pano-Azucena, O. Guillén-Fernández, and A. Silva-Juárez, 2020 *Analog/digital implementation of fractional order chaotic circuits and applications*. Springer.

Viana Jr, E. R., R. M. Rubinger, H. A. Albuquerque, A. G. de Oliveira, and G. M. Ribeiro, 2010 High-resolution parameter space of an experimental chaotic circuit. Chaos: An Interdisciplinary Journal of Nonlinear Science **20**: 023110.

Wang, R. and Z. Jing, 2004 Chaos control of chaotic pendulum system. Chaos, Solitons & Fractals **21**: 201–207.

Xu, J.-q. and G. Jin, 2012 Synchronization of parallel-connected spin-transfer oscillators via magnetic feedback.

Xu, X., M. Wiercigroch, and M. Cartmell, 2005 Rotating orbits of a parametrically-excited pendulum. Chaos, Solitons & Fractals **23**: 1537–1548.

Zhao, Y.-B., D.-Q. Wei, and X.-S. Luo, 2009 Study on chaos control of second-order non-autonomous phase-locked loop based on state observer. Chaos, Solitons & Fractals **39**: 1817–1822.

How to cite this article: Li, X., Beal, A. N., Dean, R. N., and Perkins, E. Chaos in a Pendulum Adaptive Frequency Oscillator Circuit Experiment. *Chaos Theory and Applications*, 5(1), 11-19, 2023.